CHAPTER 3

EXPERIMENTAL ASPECTS AND RESULTS

3.1 Characterisation of 'Maxon' and 'PDS II'

3.1.1 Solubility Testing

(a) Apparatus

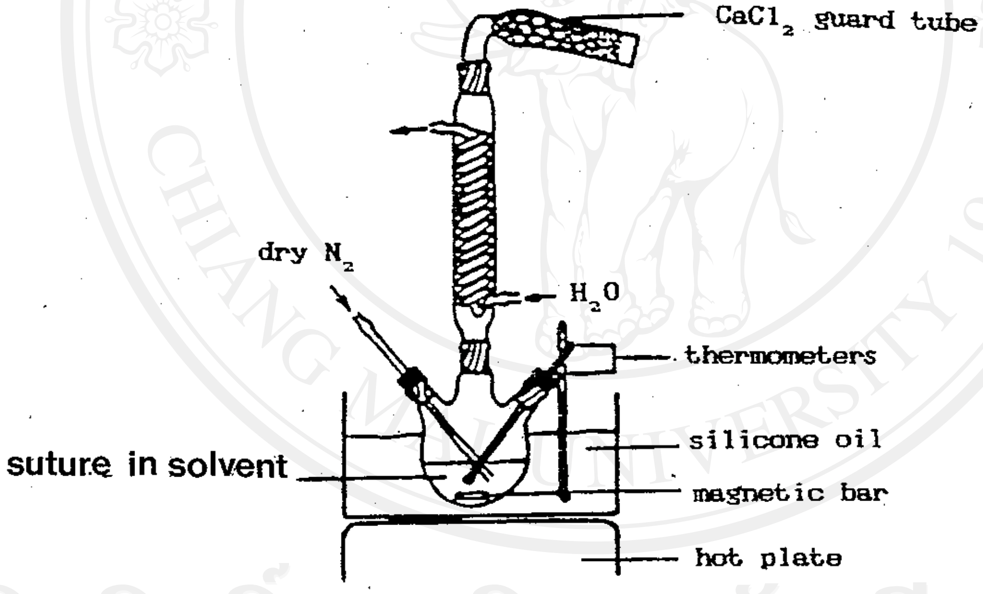

Fig. 3.1: Apparatus used for solubility testing of 'Maxon' and 'PDS II' in various solvents.

ลิขสิทธิ์มหาวิทยาลัยเชียงใหม่
Copyright© by Chiang Mai University
All rights reserved

(b) Chemicals

The chemicals used for solvent and non-solvent testing were as listed in Table 3.1.

Table 3.1: Chemicals used for solvent and non-solvent testing.

Chemicals	Chemical Formula	Grade	Supplier
'Maxon'	see below	Commercial	Davis & Geck
'PDS II'	see below	Commercial	Ethicon
Chloroform	$CHCl_3$	AR	Merck
Acetone	CH_3COCH_3	AR	BDH
Benzene	C_6H_6	AR	Merck
Benzyl alcohol	$C_6H_5CH_2OH$	AR	Merck
Carbon tetrachloride	CCl_4	AR	Merck
Dimethylsulfoxide	CH_3SOCH_3	AR	Merck
Methanol	CH_3OH	AR	Merck
Ethanol	C_2H_5OH	AR	Merck
Water	H_2O	Distilled	

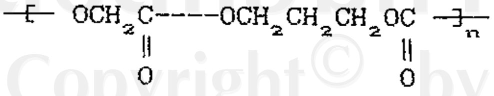

$$-\!\left[\mathrm{OCH_2\underset{\underset{O}{\|}}{C}{-}{-}{-}{-}OCH_2CH_2CH_2O\underset{\underset{O}{\|}}{C}}\right]_n\!-$$

'Maxon'

poly(glycolic acid-co-trimethylene carbonate)

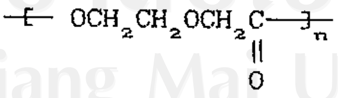

$$-\!\left[\mathrm{OCH_2CH_2OCH_2\underset{\underset{O}{\|}}{C}}\right]_n\!-$$

'PDS II'

poly-p-dioxanone

ลิขสิทธิ์มหาวิทยาลัยเชียงใหม่
Copyright © by Chiang Mai University
All rights reserved

(c) **Results**

Tables 3.2 and 3.3 show the results of solvent and non-solvent testing for 'Maxon' and 'PDS II'.

Table 3.2: Solvent testing for 'Maxon' and 'PDS II'.

Solvents	Results	
	'Maxon'	'PDS II'
Acetone	x	x
Benzene	x	x
Benzyl alcohol	✓ (125 °C)	✓ (110 °C)
Carbon tetrachloride	x	x
Dimethylsulfoxide	✓ (130 °C)	✓ (120 °C)
Chloroform	x	✓ (60 °C)
Methanol	x	x
Ethanol	x	x
Water	x	x

✓	suture dissolved completely (at minimum temperature given in parentheses)
x	suture did not dissolve, even on prolonged heating

ลิขสิทธิ์มหาวิทยาลัยเชียงใหม่
Copyright© by Chiang Mai University
All rights reserved

Table 3.3: **Non-solvent testing for 'Maxon' and 'PDS II'.**

Non-Solvents	Results (see NOTE below)	
	'Maxon'	'PDS II'
Acetone	x	x
Benzene	x	x
Carbon tetrachloride	x	x
Methanol	✓	✓
Ethanol	✓	✓
Water	(partial)	(partial)

NOTE: For both 'Maxon' and 'PDS II': from solution in hot DMSO

✓	polymer precipitated immediately and completely at room temperature as a fine white powder
x	polymer did not precipitate, even on prolonged standing in an ice-bath

ลิขสิทธิ์มหาวิทยาลัยเชียงใหม่
Copyright© by Chiang Mai University
All rights reserved

3.1.2 Melting Range Determination

A Buchi SMP-20 Melting Point Determinator was used to determine the melting ranges (T_m) of 'Maxon' and 'PDS II' by visual observation. From these determinations, the T_m ranges were found to be 200-210°C and 90-115°C respectively. These compare with ranges of 192-215°C (for 'Maxon') and 93-112 °C (for 'PDS II') obtained using a Perkin-Elmer Differential Scanning Calorimeter (Model DSC-2).

ลิขสิทธิ์มหาวิทยาลัยเชียงใหม่
Copyright© by Chiang Mai University
All rights reserved

3.2 Design and Assembly of 'In Vitro' Biodegradation Apparatus

3.2.1 Apparatus

The apparatus used for the 'in vitro' biodegradability studies was designed and assembled as shown in Fig. 3.2. The temperature inside the water bath was thermostatically controlled at 37°C (± 0.1°C) by means of a Haake (Model D3) thermocirculator.

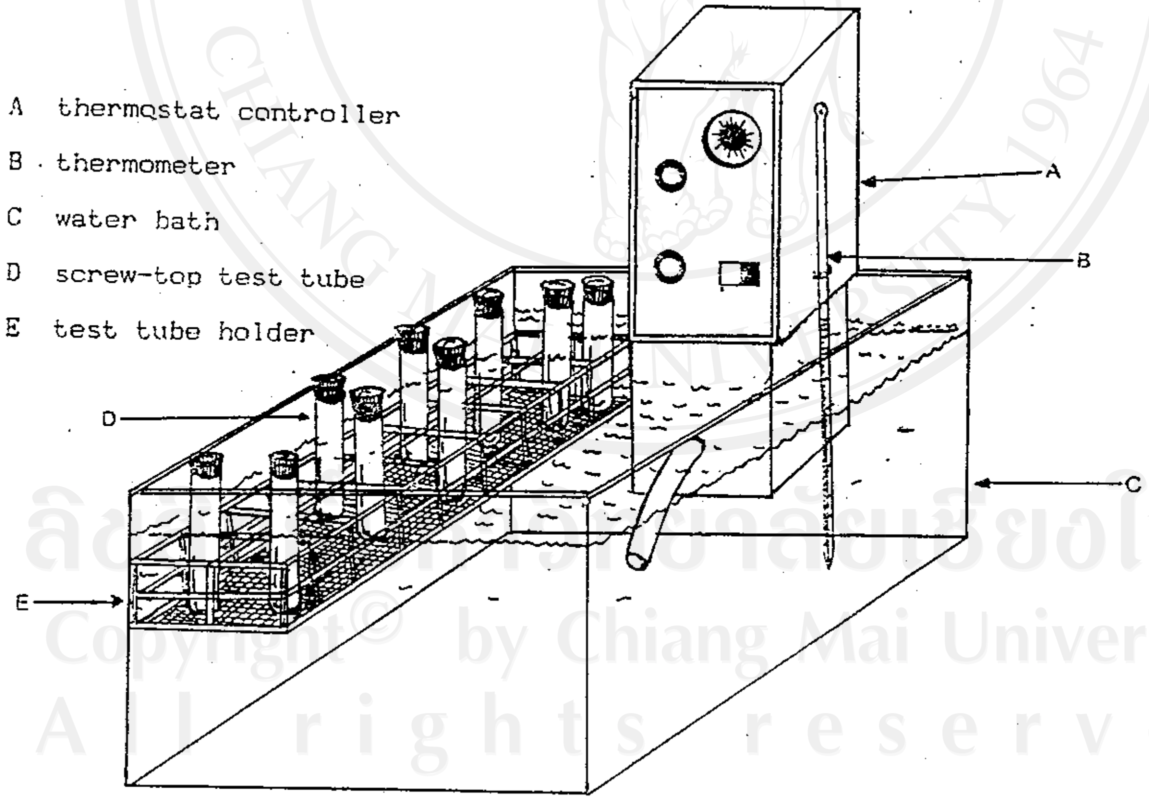

Fig. 3.2 : Apparatus used for the 'in vitro' biodegradation experiments.

ลิขสิทธิ์มหาวิทยาลัยเชียงใหม่
Copyright© by Chiang Mai University
All rights reserved

3.2.2 Chemicals

The chemicals used in the 'in vitro' biodegradation experiments were as shown in Table 3.4.

Table 3.4: Chemicals used in the 'in vitro' biodegradation experiments.

Chemicals	Grade	Supplier
SUTURES		
'Maxon' size 2-0	Commercial	Davis & Geck
'PDS II' size 2-0	Commercial	Ethicon
'Prolene' size 2-0	Commercial	Ethicon
'Ethilon' size 2-0	Commercial	Ethicon
pH BUFFER		
Di- sodium hydrogen orthophosphate anhydrous	AR	Merck
Sodium dihydrogen phosphate 2-hydrate	AR	Merck
Sodium hydroxide	AR	Merck

ลิขสิทธิ์มหาวิทยาลัยเชียงใหม่
Copyright© by Chiang Mai University
All rights reserved

3.2.3 'In Vitro' Biodegradation Procedure

All of the screw-top test tubes were sterilized before use by steam autoclaving at 100°C for 20 mins. The immersion medium was then poured into the tubes. In this work, a phosphate buffer of pH 7.40 was used as the immersion medium.

3.2.4 Preparation of Phosphate Buffer Immersion Medium

Phosphate buffer of pH 7.40 was prepared from anhydrous di-sodium hydrogen orthophosphate, Na_2HPO_4 (Salt), and sodium dihydrogen phosphate 2-hydrate, $NaH_2PO_4.2H_2O$ (Acid). From the Henderson-Hasselbach Equation :

$$pH = pK_a + \log \frac{[Salt]}{[Acid]} \qquad ...(3.1)$$

$$pH = pK_a + \log \frac{[Na_2HPO_4]}{[NaH_2PO_4.2H_2O]} \qquad ...(3.2)$$

From the " Handbook of Chemistry and Physics" [15], the pK_a of this phosphate mixture is 7.21. By calculation, 0.2 M phosphate buffer (pH 7.40) was prepared from 17.2584 g of Na_2HPO_4 and 12.2401 g

ลิขสิทธิ์มหาวิทยาลัยเชียงใหม่
Copyright© by Chiang Mai University
All rights reserved

of $NaH_2PO_4.2H_2O$ dissolved in 1 l of distilled water. The pH of the solution, which was almost 7.40, was adjusted to exactly 7.40±0.01 with 2 M NaOH.

' Maxon ' , ' PDS II ', ' Prolene ', and ' Ethilon ' sutures of size 2-0 were dried in a vacuum oven at 50 °C to constant weight and their weights accurately recorded. They were then immersed in the phosphate buffer medium in the screw-top test tubes and placed in the 37°C water bath as shown previously in Fig. 3.2. At time intervals of 1 week, one suture of each type was taken out of the medium, washed carefully with distilled water and dried to constant weight in a heated vacuum desiccator at 50 °C, as shown in Fig. 3.3. Various properties of the suture were then tested (see following Section 3.3). The experiment lasted for a total of 20 weeks.

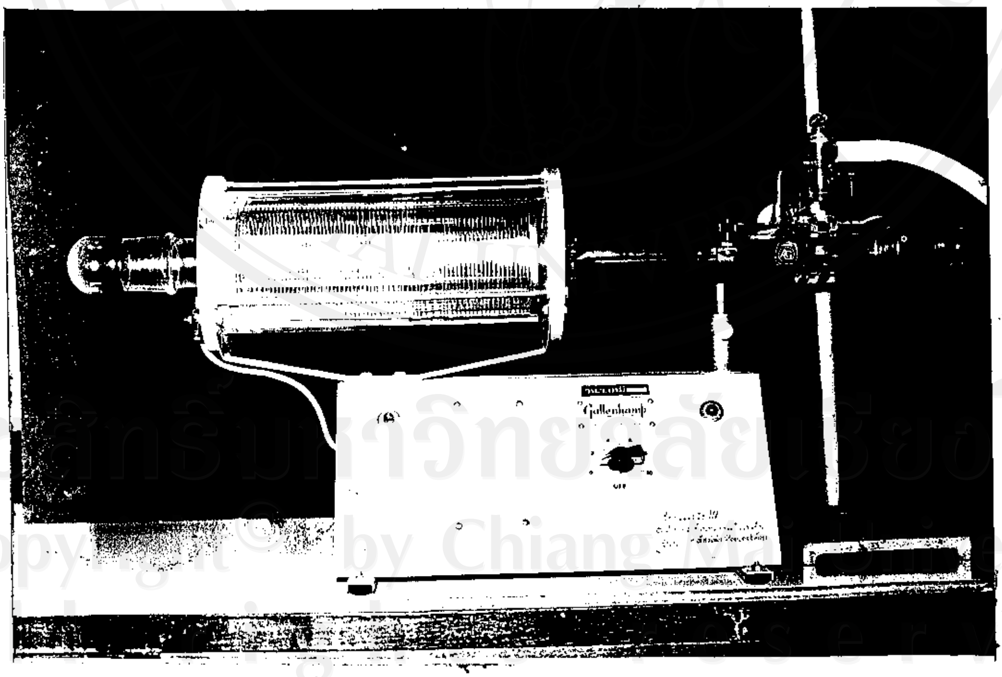

Fig. 3.3: Heated vacuum desiccator used for the efficient drying of suture samples.

ลิขสิทธิ์มหาวิทยาลัยเชียงใหม่
Copyright by Chiang Mai University
All rights reserved

3.3 Property Changes in Biodegraded 'Maxon', 'PDS II', 'Prolene' and 'Ethilon'

3.3.1 Weight Loss

An analytical balance was used to weigh the suture samples. After vacuum drying to constant weight, their % weight retentions were calculated as follows:

$$\% \text{ weight retention} = \frac{w_f \times 100 \%}{w_o}$$

where:

w_o = initial weight of sample

w_f = final weight of sample

The % weight retentions of the two absorbable sutures, 'Maxon' and 'PDS II', are shown in Table 3.5 and Fig.3.4.

The % weight retentions of the two non-absorbable sutures, 'Prolene' and 'Ethilon', are shown in Table 3.6 and Fig. 3.5.

ลิขสิทธิ์มหาวิทยาลัยเชียงใหม่
Copyright© by Chiang Mai University
All rights reserved

Table 3.5: **% Weight retentions of absorbable 'Maxon' and 'PDS II' sutures immersed in pH 7.40 phosphate buffer.**

Time (weeks)	Weight ± 0.0001 g		% Weight Retention ± 0.1	
	'Maxon'	'PDS II'	'Maxon'	'PDS II'
0	0.1909	0.2073	100.0	100.0
1	0.1909	0.2073	100.0	100.0
2	0.1909	0.2073	100.0	100.0
3	0.1905	0.2073	99.8	100.0
4	0.1904	0.2073	99.6	100.0
5	0.1888	0.2069	98.9	99.8
6	0.1875	0.2067	98.2	99.7
7	0.1855	0.2063	97.2	99.5
8	0.1825	0.2050	95.6	98.9
9	0.1726	0.2029	90.4	97.9
10	0.1613	0.2025	84.5	97.7
11	0.1541	0.1913	80.7	92.3
12	0.1468	0.1768	76.9	85.3
13	0.1434	0.1685	75.1	81.3
14	0.1346	0.1619	70.5	78.1
15	0.1285	0.1499	67.3	72.3
16	0.0960	0.1350	50.3	65.1
17	0.0903	0.1146	47.3	55.3
18	0.0584	0.1043	32.6	50.3
19	0.0575	0.0918	30.1	44.3
20	0.0573	0.0831	30.0	40.1

ลิขสิทธิ์มหาวิทยาลัยเชียงใหม่
Copyright© by Chiang Mai University
All rights reserved

Table 3.6 : **% Weight retentions of non-absorbable ' Prolene ' and 'Ethilon ' sutures immersed in pH 7.40 phosphate buffer.**

Time (weeks)	Weight ± 0.0001 g		% Weight Retention ± 0.1	
	'Prolene'	'Ethilon'	'Prolene'	'Ethilon'
0	0.1652	0.1538	100.0	100.0
2	0.1652	0.1538	100.0	100.0
4	0.1652	0.1538	100.0	100.0
6	0.1650	0.1538	99.9	100.0
8	0.1650	0.1535	99.9	99.8
10	0.1649	0.1535	99.8	99.8
12	0.1649	0.1536	99.8	99.9
14	0.1650	0.1536	99.9	99.9
16	0.1649	0.1536	99.8	99.9
18	0.1649	0.1536	99.8	99.9
20	0.1647	0.1535	99.7	99.8

ลิขสิทธิ์มหาวิทยาลัยเชียงใหม่
Copyright© by Chiang Mai University
All rights reserved

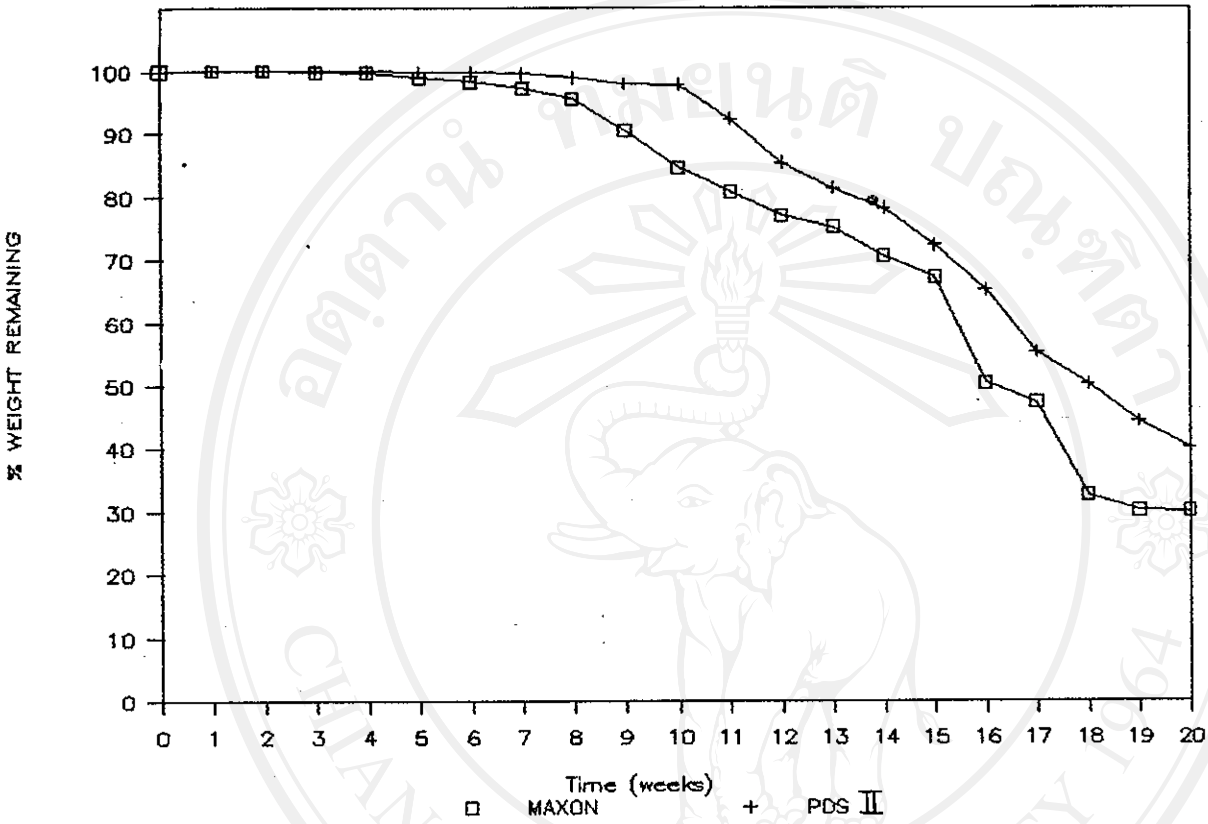

Fig 3.4 : **% Weight retentions of the two absorbable sutures, 'Maxon' and 'PDS II'.**

ลิขสิทธิ์มหาวิทยาลัยเชียงใหม่
Copyright© by Chiang Mai University
All rights reserved

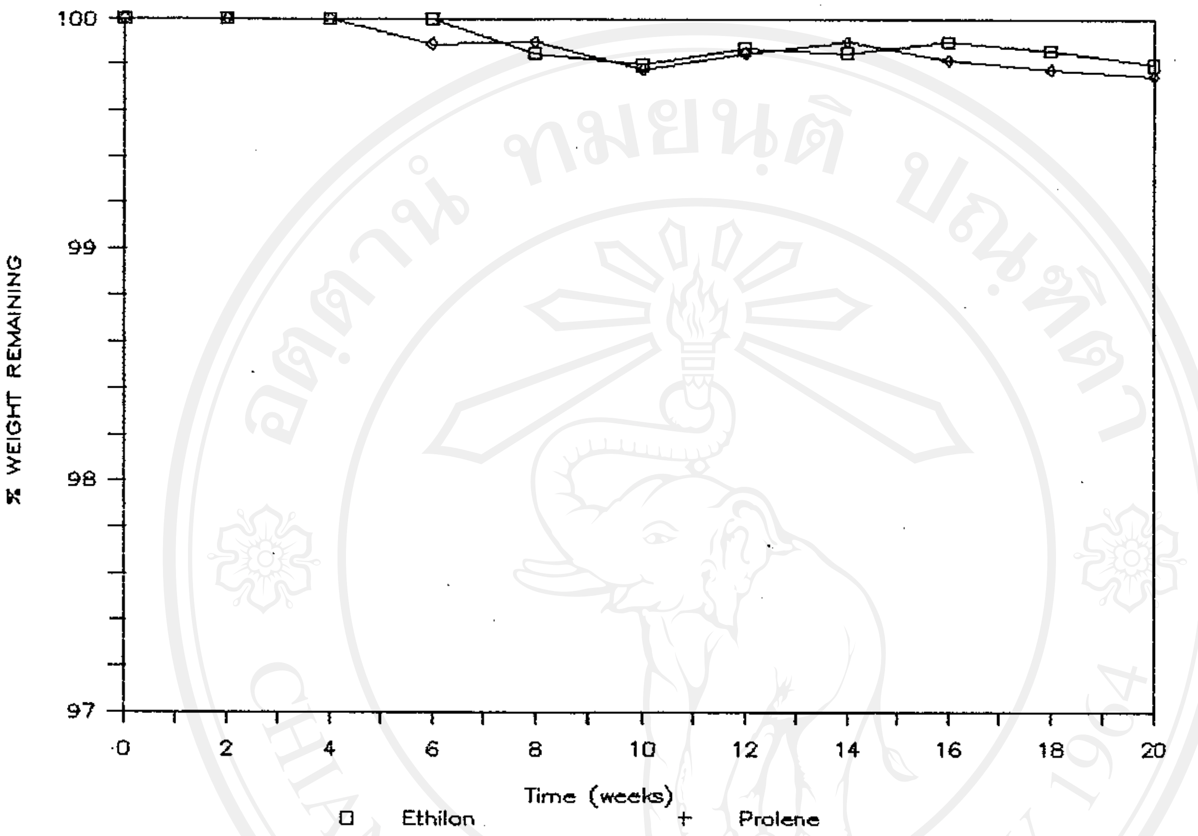

Fig.3.5 : **% Weight retentions of the two non-absorbable sutures, 'Prolene' and 'Ethilon'.**

ลิขสิทธิ์มหาวิทยาลัยเชียงใหม่
Copyright© by Chiang Mai University
All rights reserved

3.3.2 Knot Pull Force at Break

(a) Theory and Instrumentation

The knot pull force at break was measured instead of the tensile strength normally used for fiber testing. Their testing procedures are similar, except that for knot pull force testing the specimen must have a knot in the portion between the clamps [16]. Tensile strength is a maximum load (or force) based on the original cross-sectional area of the test specimen, so that it is expressed in the units of kilograms per square meter or pounds per square inch [17].

$$\text{Tensile Strength} = \frac{\text{Maximum load applied}}{\text{Cross-sectional area}} \qquad ..(3.3)$$

It has been shown experimentally that there are a number of factors which affect the tensile properties of a fiber [18]. Some of these factors are now described.

ลิขสิทธิ์มหาวิทยาลัยเชียงใหม่
Copyright© by Chiang Mai University
All rights reserved

(1) Test Specimen Length

Fig. 3.6 shows the strength or breaking load of a specimen at infinitely small increments of length along the complete length AB. If the specimen is tested at a gauge length AB, the strength recorded would be that of the weakest point and the value would be S_1. However, if the specimen is tested in two halves, two breaking loads, S_1 and S_2, are obtained, the mean of which would be higher than S_1. Hence, by testing the yarn at a shorter gauge length, the apparent yarn strength has increased. This effect is known as the "weak link" effect.

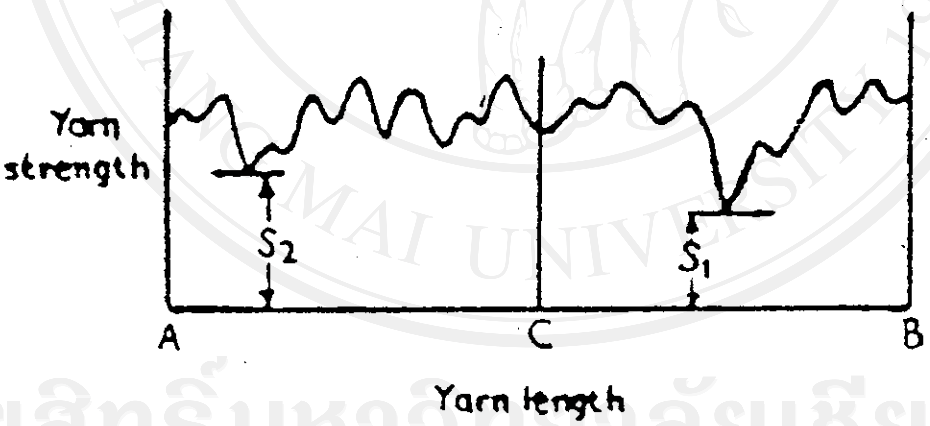

Fig. 3.6 : Fiber tensile testing: 'the weak link' effect [18].

ลิขสิทธิ์มหาวิทยาลัยเชียงใหม่
Copyright© by Chiang Mai University
All rights reserved

(2) The Rate of Loading

A rapid test procedure gives a higher breaking load than a slow test. Fig. 3.7 shows the load-extension curves produced when testing a Nylon fiber sample of 60 denier at different rates.

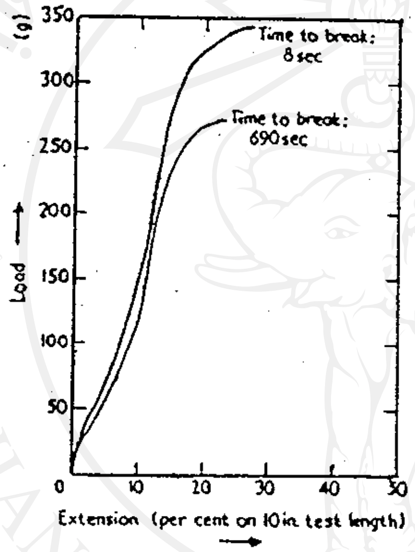

Fig. 3.7: Load-extension curves obtained at two different rates of loading for 60 denier Nylon.

(3) The Capacity of the Testing Machine

If a weak specimen is tested on a high-capacity machine, the time to break it will be short, and therefore an optimistic strength result will be produced. The capacity of the machine should be chosen so that the time required to break the specimen is close to the recommended time.

ลิขสิทธิ์มหาวิทยาลัยเชียงใหม่
Copyright© by Chiang Mai University
All rights reserved

(4) The Effect of Humidity and Temperature

The mechanical behaviour of fiber structures is influenced by the amount of moisture in the specimen. The moisture relationships of the various fiber types differ and , naturally, the degree to which the fiber properties are modified will vary. The stress-strain curve for a relatively hydrophobic material such as 'Terylene' (poly(ethylene terephthalate)) when tested in the dry state will be similar to the curve obtained from a wet test. On the other hand, the curves obtained when testing acetate rayon (cellulose acetate) dry and wet will exhibit significant differences (see Fig. 3.8). Even though a testing laboratory may have a controlled atmosphere, it is not good practice to take in samples and immediately start to test them. Sufficient time should be allowed for the samples to reach equilibrium conditions before the tests are carried out.

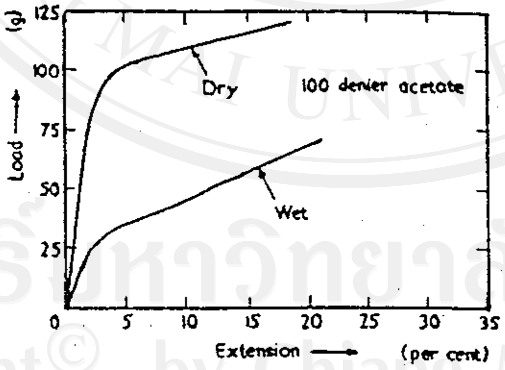

Fig. 3.8: The effect of moisture on the load-extension characteristics of 100 denier acetate rayon fiber.

ลิขสิทธิ์มหาวิทยาลัยเชียงใหม่
Copyright © by Chiang Mai University
All rights reserved

and (5) **The Previous History of the Specimen**

Chemical treatments may affect the tensile properties of the specimen. For example, damage to the fiber by chemical attack can cause serious tendering of the fiber. It is therefore desirable to know the previous history of the specimen if erroneous conclusions are to be avoided.

(b) Testing Procedure

The instrument used to determine knot pull breaking forces in this work was a Shimadzu Autograph AGS-500A Universal Testing Machine (see Fig. 3.9). A vernier was used to measure the space between the grips. Tests were carried out in an air-conditioned room under measured temperature and humidity conditions.

Each pre-dried suture specimen was cut into 10 cm lengths for testing and a double double granny knot (see Fig. 3.10) tied in the middle. The specimen was then fixed at each end in the purpose-designed screw-plates (see Fig. 3.11) and clamped between the instrument grips which were set at 5 cm apart (as measured by a vernier) . The specimens were tested under the following conditions:

ลิขสิทธิ์มหาวิทยาลัยเชียงใหม่
Copyright© by Chiang Mai University
All rights reserved

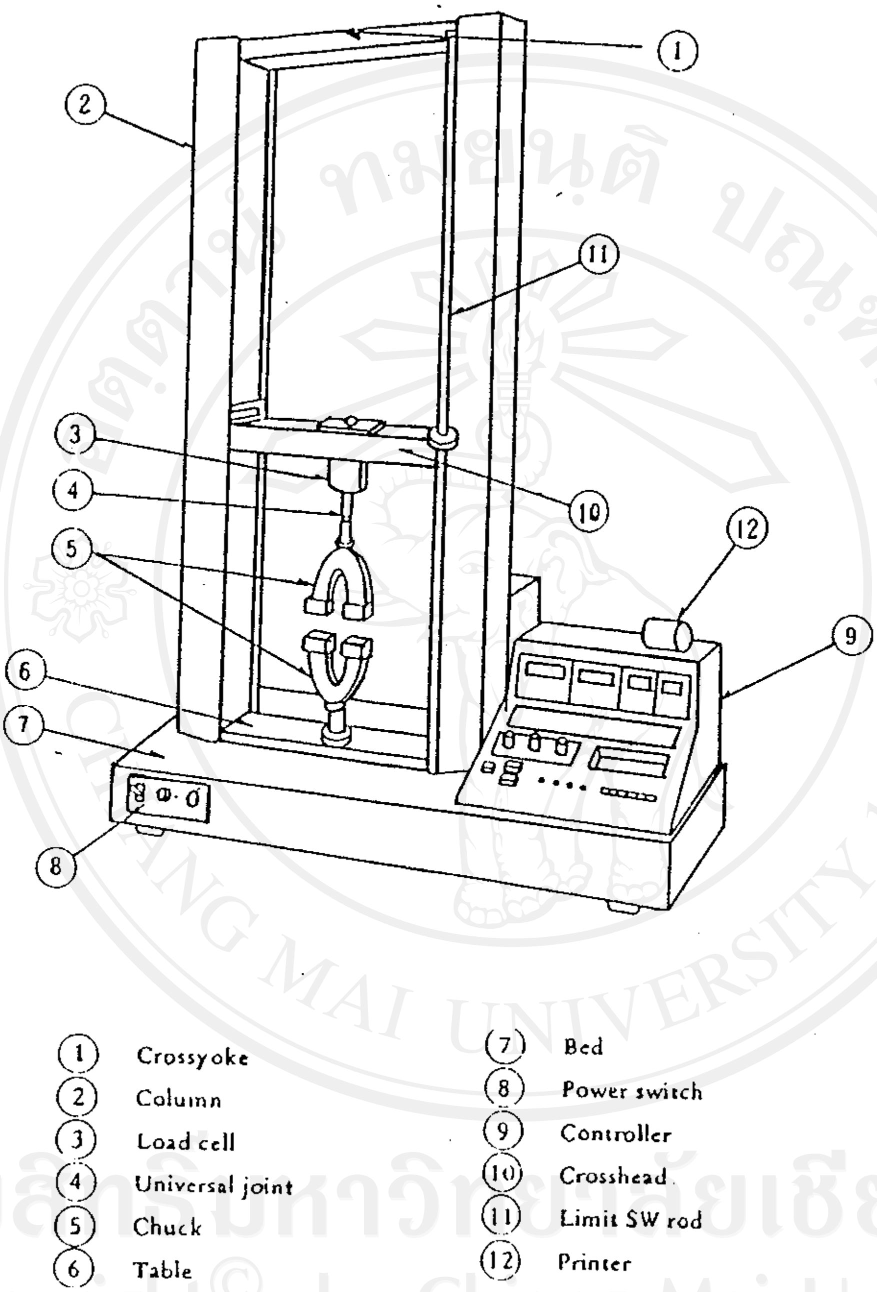

ลิขสิทธิ์มหาวิทยาลัยเชียงใหม่
Copyright© by Chiang Mai University
All rights reserved

<u>Fig. 3.9:</u> The Shimadzu Autograph AGS-500A Universal testing Machine used to determine knot pull force at break.

Load cell : 500 kgf

Load range : 50

Cross-head speed : 10 mm/min

Temperature : 26.7 °C

% Humidity : 65 %

Fig. 3.10 : A double double granny knot (2x2).

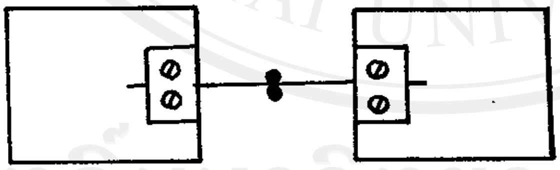

Fig. 3.11: Purpose-designed screw-plates used for specimen mounting.

ลิขสิทธิ์มหาวิทยาลัยเชียงใหม่
Copyright© by Chiang Mai University
All rights reserved

(c) Results

1. **'Maxon' and 'PDS II'**

The % knot pull breaking force retentions of the 'Maxon' and 'PDS II' samples are shown in Table 3.7 and Fig. 3.12.

Table 3.7: % Knot pull breaking force retentions of 'Maxon' and 'PDS II' sutures immersed in pH 7.40 phosphate buffer.

Times (weeks)	Average Breaking Force*, kgf		% Retention ± 0.1	
	'Maxon'	'PDS II'	'Maxon'	'PDS II'
0	3.25	3.30	100.0	100.0
1	3.24	3.09	99.7	93.7
2	3.19	2.86	98.3	86.7
3	3.16	2.41	97.4	73.0
4	3.02	1.73	93.0	52.5
5	2.92	0.80	89.9	24.4
6	2.33	0.45	73.2	13.7
7	1.70	-	52.5	-
8	0.47	-	14.7	-

* averages of at least 3 readings within ± 5%

ลิขสิทธิ์มหาวิทยาลัยเชียงใหม่
Copyright© by Chiang Mai University
All rights reserved

2. 'Prolene' and 'Ethilon'

The % knot pull breaking force retentions of the 'Prolene' and 'Ethilon' samples are shown in Table 3.8 and Fig. 3.13.

Table 3.8: % Knot pull breaking force retentions of 'Prolene' and 'Ethilon' sutures immersed in pH 7.40 phosphate buffer.

Time (weeks)	Average Breaking Force*,kgf		% Retention ± 0.1	
	'Prolene'	'Ethilon'	'Prolene'	'Ethilon'
0	2.87	3.17	100.0	100.0
2	2.86	3.11	99.8	98.1
4	2.83	3.11	98.8	98.1
6	2.78	3.04	97.0	95.9
8	2.74	2.96	95.4	93.4
10	2.74	3.00	95.4	94.7
12	2.74	2.84	95.5	89.7
14	2.72	2.87	94.8	90.5
16	2.75	2.85	95.8	89.9
18	2.77	2.86	96.5	90.3
20	2.69	2.86	93.7	90.1

* averages of at least 3 readings within ± 5 %

ลิขสิทธิ์มหาวิทยาลัยเชียงใหม่
Copyright© by Chiang Mai University
All rights reserved

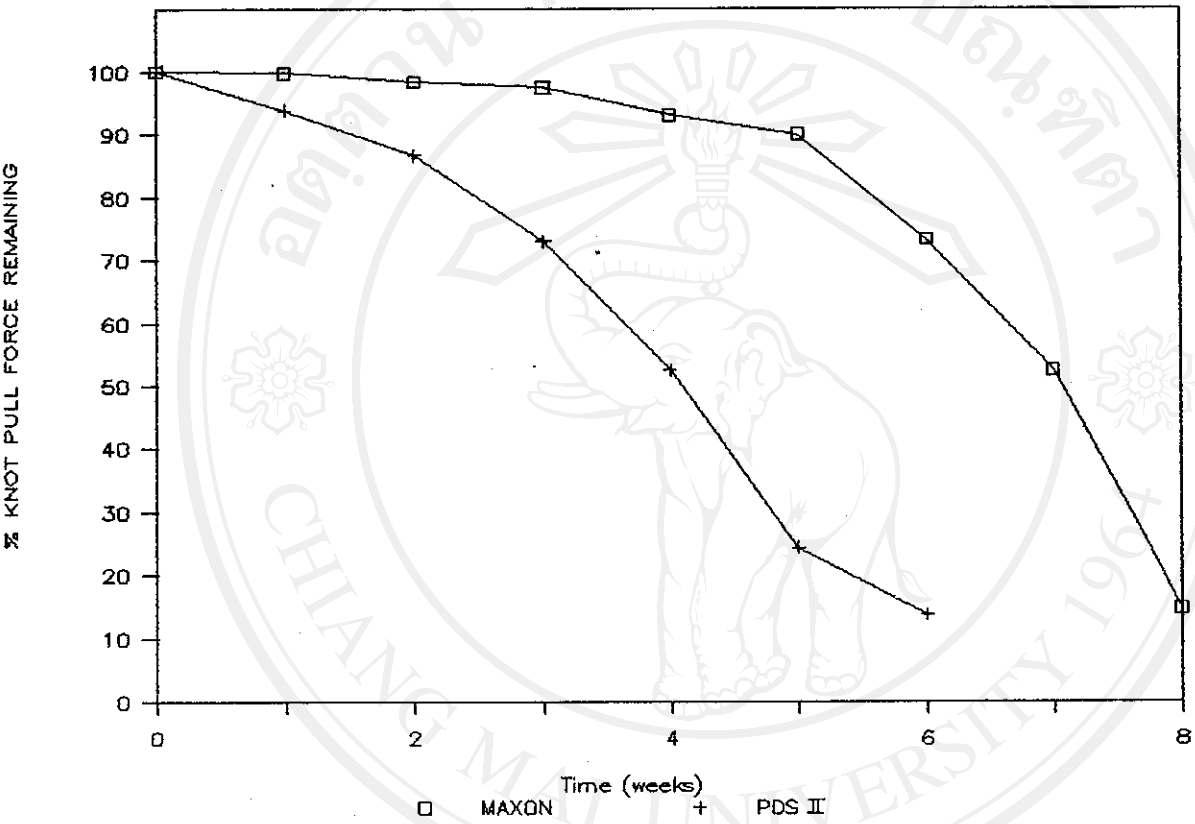

Fig. 3.12: Graphs of % knot pull breaking force retentions of 'Maxon and 'PDS II'.

ลิขสิทธิ์มหาวิทยาลัยเชียงใหม่
Copyright© by Chiang Mai University
All rights reserved

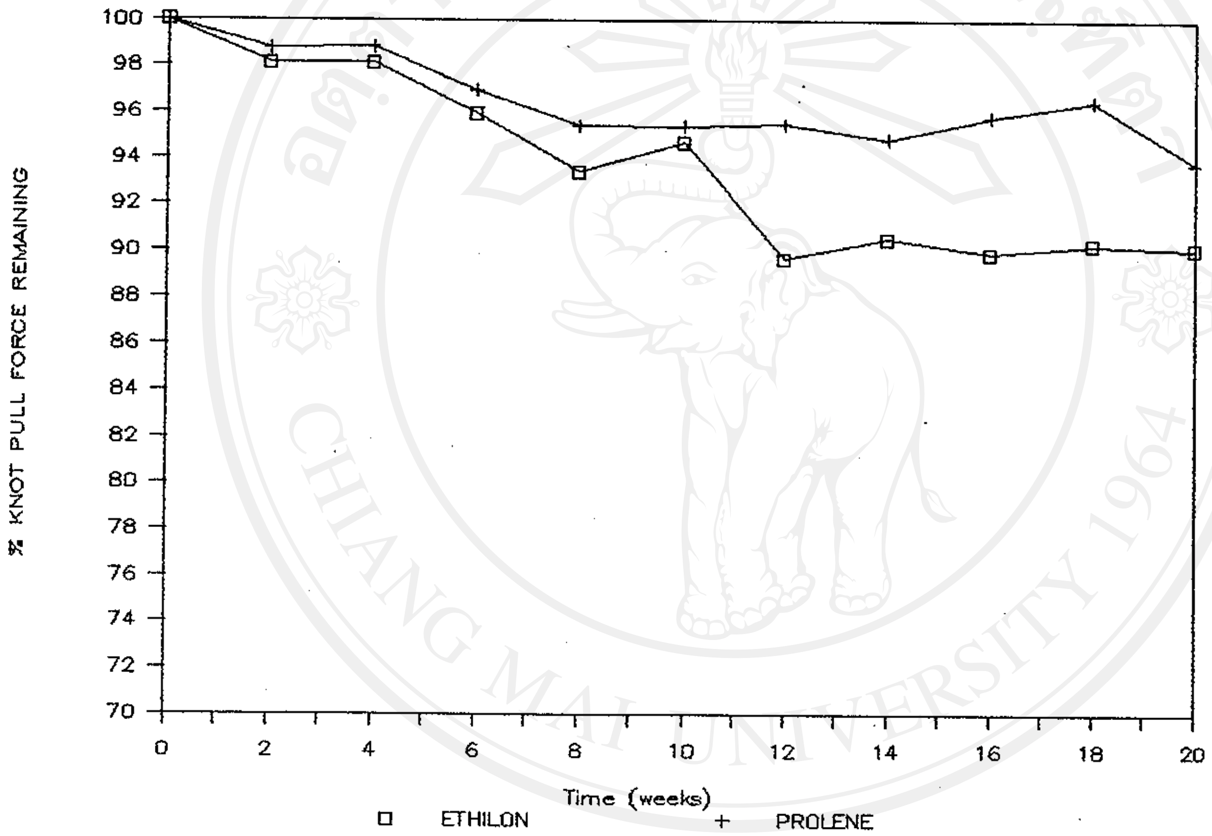

Fig. 3.13: Graphs of % Knot pull breaking force retentions of 'Prolene' and 'Ethilon'

ลิขสิทธิ์มหาวิทยาลัยเชียงใหม่
Copyright© by Chiang Mai University
All rights reserved

3.3.3 Dilute-Solution Viscometry

(a) Theory and Instrumentation

When a polymer dissolves in a liquid, the interaction of the two components stimulates an increase in polymer dimensions over that in the unsolvated state. Because of the vast difference in size between solvent and solute, the frictional properties of the solvent in the mixture are drastically altered, and an increase in viscosity occurs which should reflect the size and shape of the dissolved solute, even in dilute solutions.

One of the simplest methods of examining this effect is by capillary viscometry. The most commonly used viscometers are of the Ostwald and Ubbelohde types shown in Fig. 3.14. In the Ostwald viscometer, a given volume of liquid is introduced into B and is pumped up by gentle pressure into A until the liquid level is above the mark m_1. The pressure is released and the time required for the liquid level to fall from m_1 to m_2 is measured. The average driving force during the flow of this volume of liquid through the capillary tube is proportional to the average difference in heights of the liquid in tubes B and A (i.e., proportional to h as shown in Fig. 3.14 (a)). In order that this driving force is the same in all cases, it is clearly essential that the same amount of liquid should always be introduced into tube B. The requirement that the same amount of

ลิขสิทธิ์มหาวิทยาลัยเชียงใหม่
Copyright© by Chiang Mai University
All rights reserved

liquid should always be used does not apply in the case of the Ubbelohde viscometer (shown in Fig. 3.14(b)). Here, the liquid is introduced into B. With tube 3 closed, the liquid is pumped up into A so that the liquid level is above mark m_1. The pressure is released and, before the liquid level in tube 2 reaches the mark m_1, tube 3 is opened to the air. Bulb C fills with air and the liquid flowing out of bulb A must do so along the walls of the bulb C. In this case, the driving force for flow through the capillary is independent of the level of the liquid in B, since the average height, h, is always the same.

It has been shown that the ratio of the flow-time of the polymer solution, t, to that of the pure solvent, t_o, is effectively equal to the ratio of their viscosities (η/η_o) if the densities are considered to be approximately equal. This approximation is reasonable for dilute solutions and provides a measure of the "relative viscosity", η_r, as in equation (3.3).

$$\eta_r \quad = \quad t/t_o \quad = \quad \eta/\eta_o \qquad \ldots(3.3)$$

ลิขสิทธิ์มหาวิทยาลัยเชียงใหม่
Copyright© by Chiang Mai University
All rights reserved

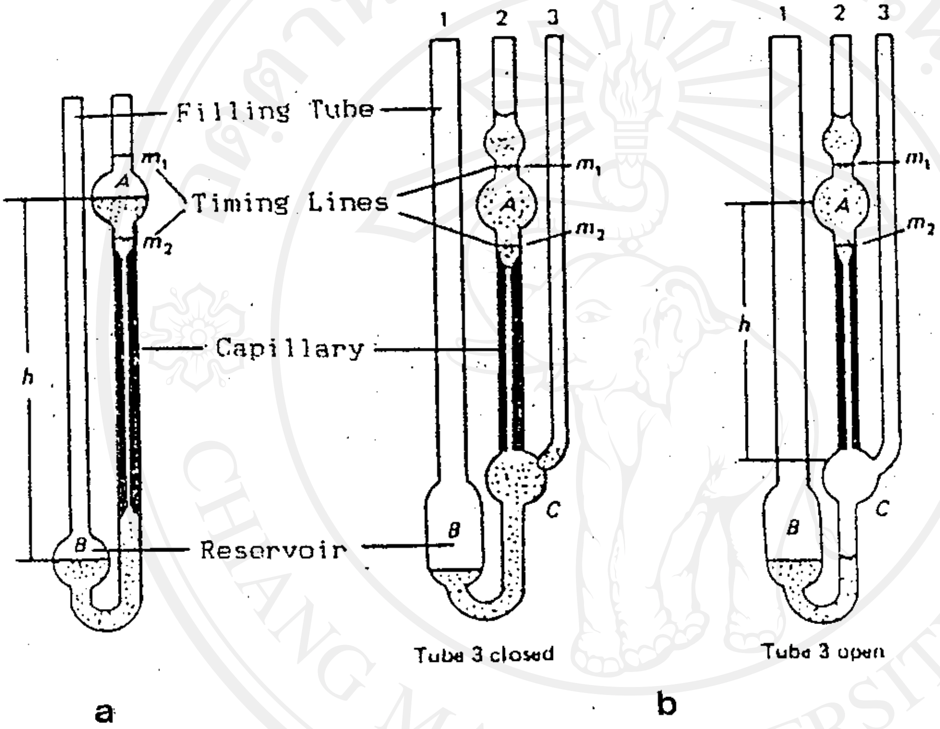

Fig. 3.14: **Dilute-solution capillary viscometers:**

(a) Ostwald, and (b) Ubbelohde types.

ลิขสิทธิ์มหาวิทยาลัยเชียงใหม่
Copyright© by Chiang Mai University
All rights reserved

Obviously, η and η_o (i.e., t and t_o) must be measured under the same conditions. The relative viscosity is always greater than unity (usually of the order of 1.1-1.5), since the presence of the polymer solute always increases the solvent viscosity. It is appropriate then to define the "specific viscosity", η_{sp} , as the fractional increase in the solvent viscosity , as shown in equation (3.4).

$$\eta_{sp} = \frac{\eta - \eta_o}{\eta_o} = \eta_r - 1 \qquad \ldots(3.4)$$

The "specific viscosity" and the "relative viscosity" depend on the concentration of the polymer in solution, increasing in magnitude with increasing concentration. Therefore, η_{sp} can be expressed as a reduced quantity called the "reduced viscosity" or "reduced specific viscosity" , $\eta_{red} = \eta_{sp}/c$. The "reduced viscosity" at which the concentration approaches zero is called the "intrinsic viscosity", $[\eta]$, and is given by:

$$[\eta] = (\eta_{sp}/c)_{c=0} \qquad \ldots(3.5)$$

It is this intrinsic viscosity term, $[\eta]$, which is related to the polymer's average molecular weight. Alternative methods of calculating $[\eta]$ are now described.

ลิขสิทธิ์มหาวิทยาลัยเชียงใหม่
Copyright© by Chiang Mai University
All rights reserved

(i) Huggins-Kraemer Method

The intrinsic viscosity, $[\eta]$, is most commonly and conveniently determined via the Huggins Equation [**19**]

$$\eta_{sp}/c \quad = \quad [\eta] + k'[\eta]^2 c \qquad \ldots(3.6)$$

and the Kraemer Equation [**20**]

$$(\ln \eta_r) / c \quad = \quad [\eta] + k'' [\eta]^2 c \qquad \ldots(3.7)$$

Here, the term $(\ln \eta_r) / c$ is usually referred to as the "inherent viscosity", η_{inh} , and k' and k'' are constants for a given polymer-solvent system at a given temperature and are themselves mathematically related by equation (3.8).

$$k' - k'' \quad = \quad 0.5 \qquad \ldots(3.8)$$

The value of k' is usually in the range $0.3 < k' < 0.5$ and increases as solvent power decreases.

Thus, the two equations (3.6) and (3.7) should yield linear plots against concentration, c, with their common intercept equal to $[\eta]$ at c=0, as shown in Fig. 3.15. The double extrapolation facilitates the accurate estimation of $[\eta]$.

ลิขสิทธิ์มหาวิทยาลัยเชียงใหม่
Copyright© by Chiang Mai University
All rights reserved

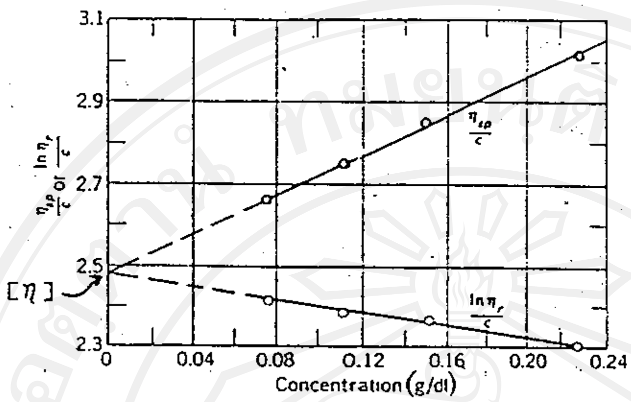

Fig. 3.15: **Reduced and inherent viscosity - concentration plots for a typical polymer sample.**

Good straight line graphs are usually obtained when the concentration of the solutions measured is not too large (i.e., < 1 % w/v), thus avoiding intermolecular forces and chain entanglement effects between polymer molecules of very high molecular weight.

(ii) Solomon - Ciuta One-point Approximation Method [21]

Measurement of the solution viscosity at only a single concentration can also enable calculation of the intrinsic viscosity from the Solomon-Ciuta Equation [21].

ลิขสิทธิ์มหาวิทยาลัยเชียงใหม่
Copyright© by Chiang Mai University
All rights reserved

$$[\eta] = [\, 2(\eta_{sp} - \ln\eta_r)]^{1/2} \;/\; c \qquad \ldots(3.9)$$

This equation is obtained by combination of the previous equations (3.6), (3.7) and (3.8) followed by elimination of k' and k''. However, this method is accurate only when it is already known that there is a good linear relationship between c and η_{sp} / c and /or $(\ln\eta_r)/c$. This is the method that was used in this work for determination of $[\eta]$.

The intrinsic viscosity, $[\eta]$, is related to the polymer molecular weight by the Mark-Houwink-Sakurada Equation [**22**–**23**]

$$[\eta] = K\, M_v^{\,a} \qquad \ldots(3.10)$$

where:

K and a are constants for the polymer-solvent pair at a given temperature and are usually obtained from the "Polymer Handbook" [**24**].

M_v is the so-called "viscosity-average molecular weight".

ลิขสิทธิ์มหาวิทยาลัยเชียงใหม่
Copyright© by Chiang Mai University
All rights reserved

(b) Experimental Procedure

Approximately 0.25 % w/v 'Maxon' and 'PDS II' suture solutions were accurately prepared using dimethylsulfoxide (DMSO) as solvent. The solutions were prepared by heating to 130°C and 125°C for 'Maxon' and 'PDS II' respectively under nitrogen (see Fig. 3.16). Their flow-times were then determined at 100 °C using a Schott-Gerate micro-Ubbelohde viscometer (type 537 10, capillary size I), as part of the overall system shown in Fig. 3.17. Using the One-point Approximation Method (see previous section), the intrinsic viscosities, $[\eta]$, were calculated as given in Table 3.19 and Fig. 3.18.

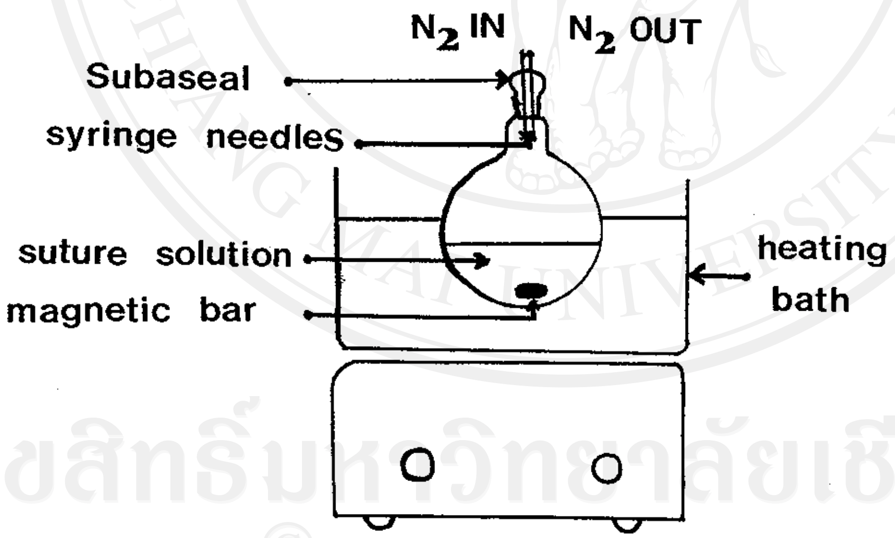

ลิขสิทธิ์มหาวิทยาลัยเชียงใหม่
Copyright© by Chiang Mai University
All rights reserved

Fig. 3.16 : The apparatus used for dissolving 'Maxon' and 'PDS II' for dilute-solution viscosity measurements.

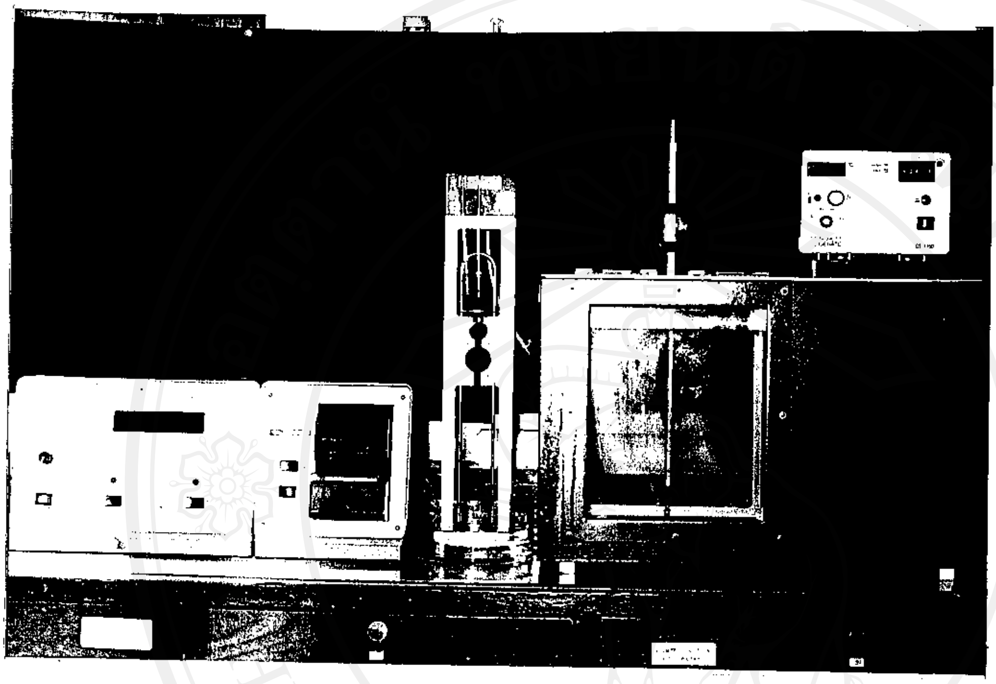

Fig. 3.17: Schott-Gerate AVS 300 Automatic Viscosity Measuring System.

ลิขสิทธิ์มหาวิทยาลัยเชียงใหม่
Copyright© by Chiang Mai University
All rights reserved

Table 3.9: Intrinsic viscosities and their % retentions for 'Maxon' and 'PDS II' sutures immersed in pH 7.40 phosphate buffer.

Time (weeks)	[η] , ± 0.01 dl/g		% Retention ± 0.1	
	'PDS II'	'Maxon'	'PDS II'	'Maxon'
0	0.49	0.58	100.0	100.0
1	0.40	0.51	81.8	87.3
3	0.28	0.44	57.8	75.3
5	0.20	0.38	40.9	66.3
7	0.10	0.29	21.3	50.3
9	0.05	0.17	10.2	30.2
11	-	0.15	-	20.3
13	-	0.09	-	15.2

ลิขสิทธิ์มหาวิทยาลัยเชียงใหม่
Copyright© by Chiang Mai University
All rights reserved

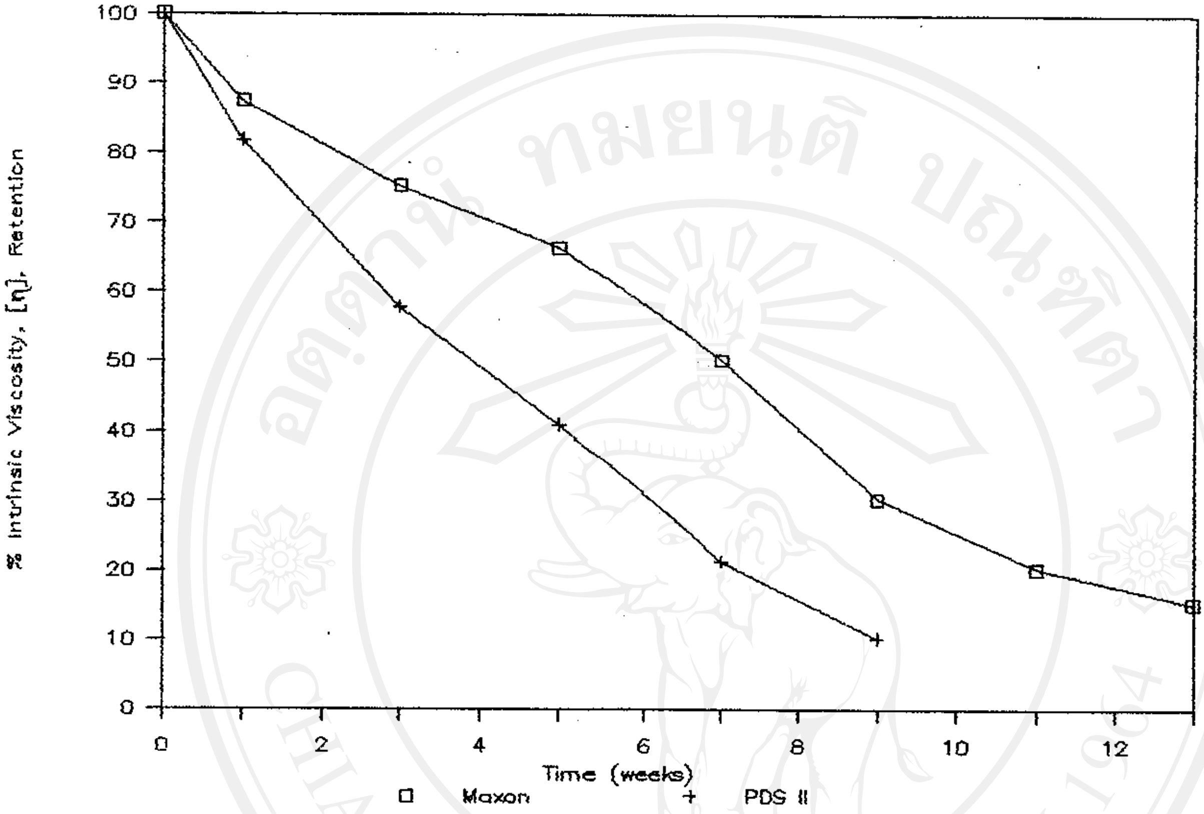

Fig 3.18: Changes in % retentions of intrinsic viscosity, [η], of 'Maxon' and 'PDS II' sutures with time of immersion in pH 7.40 phosphate buffer.

ลิขสิทธิ์มหาวิทยาลัยเชียงใหม่
Copyright© by Chiang Mai University
All rights reserved